Ciencia en Desarrollo, Vol. 8 No. 1
ISSN 0121-7488 – Enero-Junio de 2017, pp. 109-117

Methylene blue degradation over M-TiO_2 photocatalysts (M= Au or Pt)

Degradación de azul de metileno sobre fotocatalizadores M-TiO_2 (M = Au o Pt)

Julie Joseane Murcia Mesa [a]*
Jhonatan Ricardo Guarín Romero [a]
Ángela Carolina Cely Macías [a]
Hugo Alfonso Rojas Sarmiento [a]
Jairo Antonio Cubillos Lobo [a]
María del Carmen Hidalgo López [b]
José Antonio Navío Santos [b]

Recepción: 6 de septiembre de 2016
Aceptación: 30 de diciembre de 2016

Abstract

In this study it was evaluated the methylene blue degradation over TiO_2 modified by sulfation and Au or Pt addition. These materials were synthesized by photodeposition method and then were widely characterized by different techniques. In general, it was found that Au or Pt particles size distribution can be effectively controlled modifying the deposition time. It was also found that metal particle size and dye adsorption on TiO_2 surface, are important factors influencing the methylene blue degradation rate. The highest dye degradation was obtained on Au-S-TiO_2 photocatalyst prepared by using 120 min of deposition time; the highest effectiveness of this material in the methylene blue degradation can be mainly due to a combined effect between the presence of gold nanoparticles acting as a sink for the electrons photogenerated during the catalytic reaction and the better adsorption of the dye over the S-TiO_2 surface partially covered by gold particles with the largest sizes.

Keywords: Methylene blue, photodegradation, sulfated TiO_2, M-TiO_2, photocatalysts.

Resumen

En este estudio se evaluó la degradación de azul de metileno sobre TiO_2 modificado por sulfatación y adición de Au o Pt. Estos materiales fueron sintetizados a través del método de fotodeposición y caracterizados usando diferentes técnicas. En general, se encontró que la distribución de tamaño de partícula de Au o Pt se puede controlar efectivamente modificando el tiempo de fotodeposición. Se encontró también que factores como el tamaño de partícula metálica y la adsorción del colorante sobre la superficie del TiO_2 influencian de manera importante la velocidad de degradación del azul de metileno. La mayor degradación del colorante se obtuvo usando el fotocatalizador Au-S-TiO_2 preparado con un tiempo de deposición de 120 min; la alta efectividad de este material en la degradación del azul de metileno se debe principalmente a un efecto combinado entre la presencia de partículas de oro que actúan como colectores de los electrones fotogenerados durante la reacción catalítica y a la mejor adsorción del colorante sobre la superficie del S-TiO_2 cubierta parcialmente por partículas de oro con el mayor tamaño.

Palabras claves: Azul de metileno, fotodegradación, FOTOCATALISIS, M-TiO_2, TiO_2 sulfatado.

[a] Grupo de Catálisis, Escuela de Ciencias Químicas, Universidad Pedagógica y Tecnológica de Colombia UPTC, Avenida Central del Norte, Tunja, Boyacá, Colombia.
* Autor de Correspondencia: jmurciamesa5@gmail.com
[b] Instituto de Ciencia de Materiales de Sevilla (ICMS), Consejo Superior de Investigaciones Científicas CSIC - Universidad de Sevilla, Américo Vespucio 49, 41092 Seville, Spain.

1. Introduction

Solving environmental problems represent a challenge for the scientific community around the world, to address these issue different alternatives have been employed, these have been mainly focused on the synthesis of new materials and all of them are based on the principles of the green chemistry [1-3].

Currently, dyestuffs coming from textile and food industries are important pollutants in aqueous effluents. These dyes represent a serious problem for human and animal health; for that reason the degradation of these pollutants have acquired increasing attention in the last decade. For the wastewater treatment, have been employed many physical and chemical methods [1], these methods can be expensive or in many cases ineffective. Currently, heterogeneous photocatalysis based on TiO_2 has demonstrated to be an effective and easy treatment of water sources polluted with dyes [5-7].

Due to their many advantages, TiO_2 is the main semiconductor used in photocatalytic processes; however this oxide has some limitations related to the higher electron-hole recombination and lower activity under visible light. In order to improve its photocatalytic activity, many strategies such as sulfation and noble metal addition have been employed [8-10]. The oxygen vacancies generated on the sulfated titania and the presence of metal nanoparticles decreases the electron-hole recombination, thus improving the TiO_2 efficiency in the photodegradation reactions. It has been reported that the improvement of TiO_2 photoactivity by noble metal addition depends not only on metal content but also on TiO_2 properties, metal particle size and metal oxidation state [8-13]. So, it is very important to control the synthesis parameters in order to obtain highly effective photocatalysts based on modified TiO_2 [14].

The main objective of this work was to prepare photocatalysts based on TiO_2 modified by simultaneous processes of sulfation and noble metal photodeposition. The materials thus obtained were evaluated in the methylene blue photodegradation reaction. The effect of the noble metal Au or Pt and the metal particle size on the effectiveness of the photoreaction was also evaluated.

2. Materials and methods

2.1 Synthesis of M-TiO_2 photocatalysts

In a typical procedure TiO_2 used as starting material was prepared by the hydrolysis of titanium tetraisopropoxide (Aldrich, 97%) in isopropanol solution (1.6 M) by the slow addition of distilled water (volume ratio isopropanol/water 1:1). Afterward, the generated precipitate was filtered, dried at 110°C overnight and calcined at 650 °C for 2h. Sulfation treatment was applied to TiO_2 before calcination; the powders were sulfated by immersion in H_2SO_4 aqueous solution 1 M for 1 h and afterward calcinated at 650 ºC for 2 h. Sulfation treatment was carried out for two reasons; on one hand, previous results have shown that sulfation stabilizes the anatase phase up to high temperatures and protect the catalyst from the loss of surface area by sintering [15-17]. On the other hand, at the calcination temperature of 650 ºC, the elimination of sulfate groups promotes the creation of high number of oxygen vacancies, which have been reported as preferential sites for noble metal adsorption [18].

The sulfated TiO_2 (S-TiO_2) was modified by noble metal addition (gold or platinum), using the photodeposition method. Gold (III) chloride trihydrate ($HAuCl_4.3H_2O$, Aldrich 99.9%) or hexachloroplatinic acid (H_2PtCl_6, Aldrich 99.9%) were used as metal precursors for Au and Pt, respectively. Under an inert atmosphere (N_2), a suspension of sulfated TiO_2 in distilled water containing isopropanol (Merck 99.8%) which acts as sacrificial donor was prepared. Then, the appropriate amount of metal precursor to obtain a nominal Au or Pt loading of 0.5% weight total to TiO_2 was added; this nominal weight was selected for this work, taking into account that in previous studies it has been reported that by using this noble metal content it is possible to achieve a suitable effectiveness in the elimination of different organic pollutants including dyes in liquid phase [6,8,15,16]. Final pH of the suspensions was 3. Photochemical deposition of Au or Pt was then performed by illuminating the suspensions with an Osram Ultra-Vitalux lamp (300W) with a sun-like radiation spectrum and a main emission line in the UVA range at 365 nm, using two different illumination times of 15 and 120 min. The light intensity on the TiO_2 surface was 140 W/m^2. After photodeposition, the powders were recovered by filtration and dried at 110 °C overnight. The metallized samples were labeled as Au-S-TiO_2 and Pt-S-TiO_2.

2.2. Characterization of the M-TiO_2 photocatalysts

BET surface areas (S_{BET}) of all samples were evaluated by N_2 adsorption measurement with a Micromeritics ASAP 2010 instrument.

Degasification of the samples was performed at 150 ºC for 30 min in He flow.

Crystalline phase composition and degree of crystallinity of the samples were estimated by X-ray diffraction (XRD). XRD patterns were obtained on a Siemens D-501 diffractometer with Ni filter and graphite monochromator using Cu Kα radiation. Crystallite sizes were calculated from the line broadening of the main anatase X-ray diffraction peak (1 0 1) by using the Scherrer equation. Peaks were fitted by using a Voigt function.

Chemical composition and total platinum and gold content in the samples were determined by X-ray fluorescence spectrometry (XRF) in a Panalytical Axios sequential spectrophotometer equipped with a rhodium tube as the source of radiation. XRF measurements were performed onto pressed pellets (sample included in 10 wt.% of wax).

The morphology for all the samples was analyzed by field Scanning electron microscopy (SEM) using a Hitachi S 4800 microscope. Transmission electron microscopy (TEM) was performed in a Philips CM 200 microscope. The samples for the microscopic analyzes were dispersed in ethanol using an ultrasonicator and dropped on a carbon grid.

Light absorption properties of the samples were studied by UV–Vis spectroscopy. The Diffuse Reflectance UV–Vis Spectra (UV–Vis DRS) were recorded on a Varian spectrometer model Cary 100 equipped with an integrating sphere and using $BaSO_4$ as reference. Band-gaps values were calculated from the corresponding Kubelka–Munk functions, $F(R\infty)$, which are proportional to the absorption of radiation, by plotting $(F(R\infty) \times h\upsilon)^{1/2}$ against $h\upsilon$.

X-ray photoelectron spectroscopy (XPS) studies were carried out on a Leybold-Heraeus LHS-10 spectrometer, working with constant pass energy of 50 eV. The spectrometer main chamber, working at a pressure $<2\times10^{-9}$ Torr, is equipped with an EA-200 MCD hemispherical electron analyzer with a dual X-ray source working with Al Kα ($h\upsilon$ = 1486.6 eV) at 120 W and 30 mA. C 1s signal (284.6 eV) was used as internal energy reference in all the experiments. Samples were outgassed in the pre-chamber of the instrument at 150 ºC up to a pressure $<2\times10^{-8}$ Torr to remove chemisorbed water.

2.3. Methylene blue photodegradation tests

The photocatalytic activity of the catalysts prepared was tested in the degradation of methylene blue (MB). Photocatalytic tests were carried out by using a discontinuous batch system, this includes a 400 mL pyrex reactor enveloped by an aluminum foil, filled with an aqueous suspension (250 mL) containing 25 ppm of MB and the photocatalyst (1 g/L). This system was illuminated through a UV-transparent Plexiglas® top window (threshold absorption at 250 nm) by an Osram Ultra-Vitalux lamp (300 W) with sun-like radiation spectrum and a main line in the UVA range at 365 nm. The intensity of the incident UV-Visible light on the solution was measured with a Delta OHM photoradiometer HD2102.1, being ca. 120 W/m^2. In order to favor the adsorption–desorption equilibrium, prior to irradiation the suspension was magnetically stirred for 10 min in dark. Magnetic stirring and a constant oxygen flow of 25 L/h as an oxidant were used to produce a homogeneous suspension of the photocatalyst in the solution. A bubbler tank was used as a source of natural oxygen. All photocatalytic tests started at pH ca. 4.0 and the total reaction time was 120 min.

During the MB photoreaction, samples were collected at different times and in order to evaluate the dye discoloration rate, the concentration of MB during the photodegradation reaction was analyzed by UV–Visible spectroscopy, considering the main peak of this dye located at 665 nm. For this analysis it was used a Genesis series 10 GBC 911 instrument.

Photolysis tests of MB under UV-Visible light and in absence of catalyst were also carried out. Under the experimental conditions used in this work, substrate photolysis was negligible. Reproducibility of the measurements was ensured by double testing of selected samples.

Dye degradation rate was calculated for each photoreaction, by using the equation 1.

$$v = k * Co * V \qquad \text{(Equation 1)}$$

Where:

v = Degradation rate
k = calculate from the slope of the graph representing MB concentration Vs reaction time.
Co = Initial concentration of MB (mol/L)
V = Volume of MB (L)

3. Results and discussion

3.1 Characterization of M-TiO_2 photocatalysts

A summary of the characterization results is presented in Table 1, and these results are discussed and analyzed as follows.

Table 1. Summary of the characterization results.

Catalyst	Deposition time (min)	$D_{Anatase}$ (nm)	S_{BET} (m^2/g)	Band gap (eV)	Binding energy (eV)	
					Ti $2p_{3/2}$	O 1s
Bare TiO_2	-	11	17	3.30	458.5	529.8
S-TiO_2	-	20	58	3.20	458.5	529.8
Au-TiO_2	15	21	54	3.20	459.6	530.8
	120	20	53	3.21	458.8	530.1
Pt-TiO_2	15	23	53	2.80	458.5	529.9
	120	21	59	2.80	458.4	529.6

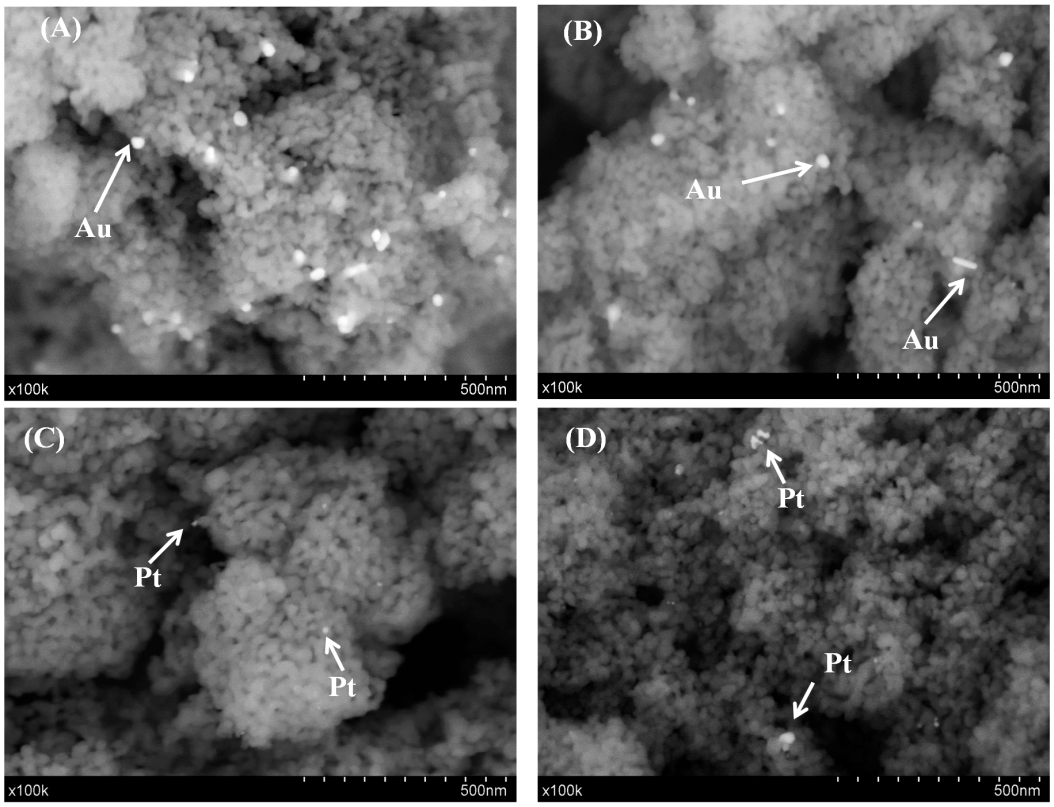

Figure 1. SEM images of S-TiO_2 modified by Au or Pt deposition using different deposition times. (A) Au-S-TiO_2 at 15min; (B) Au- S-TiO_2 at 120min; (C) Pt- S-TiO_2 at 15min and (D) Pt- S-TiO_2 at 120min.

The specific surface area of the unmodified titania (bare TiO_2) photocatalyst was measured by N_2 physisorption at -196 °C and it was found to be 11 m^2/g; after sulfation (S-TiO_2), this value considerably increases, this is mainly due to the protective effect of this treatment during the calcination processes. After Au or Pt addition the S_{BET} slightly decreases to values between 53 – 54 m^2/g, it could be due to the pore obstruction by the metal particles.

By XRD only peaks ascribed to anatase phase were detected in all the samples analyzed. The anatase crystallite size for sulfated TiO_2 was 20 nm, metal addition or time used in the photodeposition of the metals on S-TiO_2 surface did not induce any important modification on this parameter.

The metal content in the samples was determined by X-ray fluorescence and it was found that in all the samples the metal (gold or platinum) content was under the nominal value (0.5 wt.%), thus indicating the incomplete reduction of the metal precursors during the synthesis. In the case of the samples prepared with 15 minutes of photodeposition the contents of gold and platinum were 0.36% and 0.26%, respectively. The increase of the deposition time also increases the metal content, thus in the photocatalysts synthesized with 120 min of deposition time, metal contents of 0.45% and 0.41% were observed for Au-S-TiO_2 and Pt-S-TiO_2 samples, respectively.

The morphology, distribution and size of the Au and Pt nanoparticles on S-TiO_2 were studied by SEM and TEM microscopies and selected images obtained for the metallized samples are presented in Figure 1 and 2, respectively. As it can be observed in Figure 1, gold particles are larger than platinum particles,

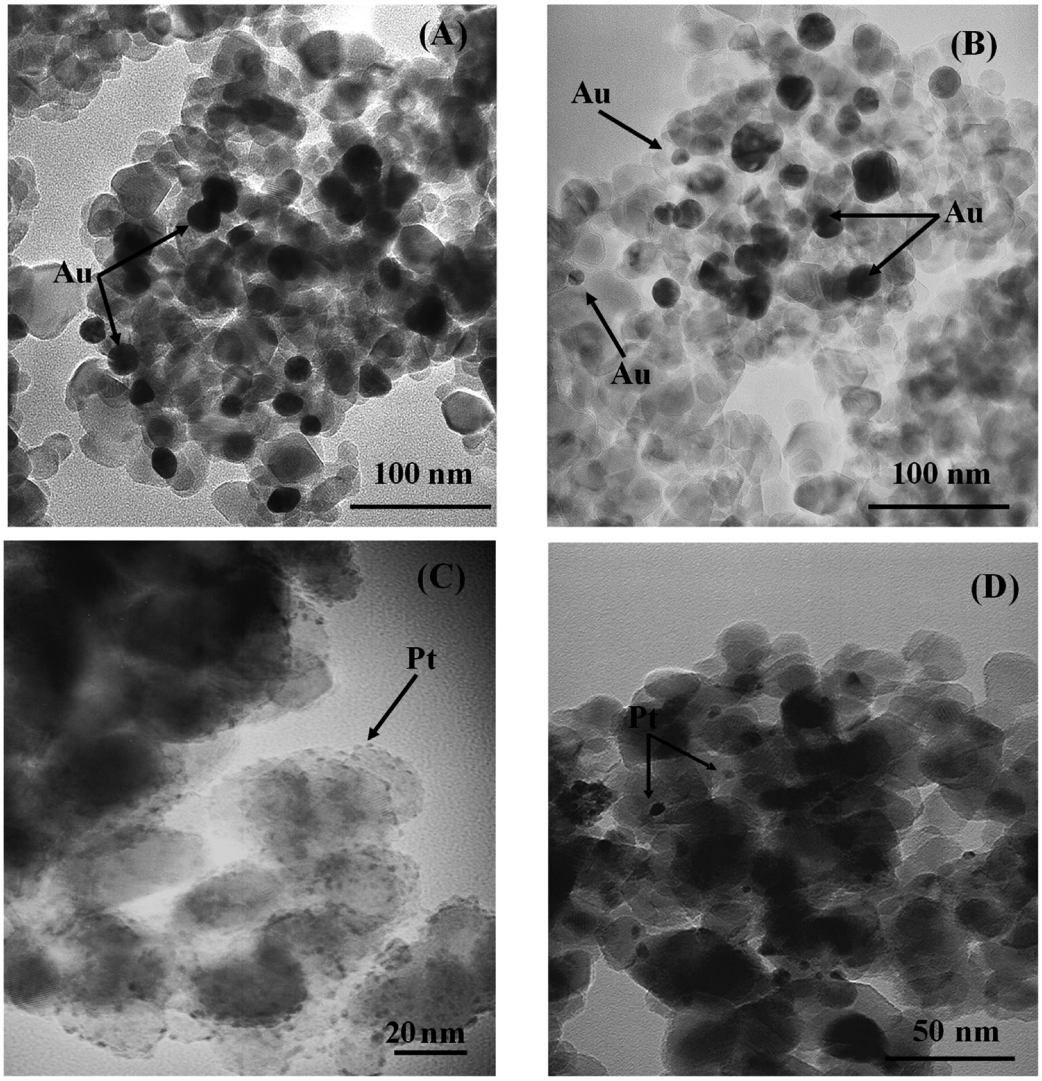

Figure 2. TEM images of S-TiO_2 modified by Au or Pt deposition using different deposition times. (A) Au- S-TiO_2 at 15min; (B) Au- S-TiO_2 at 120min; (C) Pt- S-TiO_2 at 15min and (D) Pt- S-TiO_2 at 120min.

also it is possible to observe that in the metallized samples the number of metal particles deposited on S-TiO_2 surface increases with the deposition time (from 15 until 120 min).

The metal particles sizes were determined by TEM analysis. Selected TEM images of Au-S-TiO_2 and Pt-S-TiO_2 samples prepared with different deposition times are presented in Figure 2; in these images black dots can be identified as gold or platinum deposits. Figure 2A shows an image of the catalyst Au-S-TiO_2 prepared at 15 min of deposition time, as it can be seen gold particles are between 20 and 40 nm; these particles are heterogeneously distributed over S-TiO_2 surface with places with a high concentration of gold deposits and others relatively empty. In the case of the sample prepared at 120 min of deposition time (Figure 2B), it is possible to observe that the gold particle size increases to with average sizes between 40 and 50 nm; smallest particles with sizes less than 20 nm were also found in this sample.

Figures 2C and 2D show selected images of Pt-S-TiO_2 samples prepared at 15 and 120 min of deposition times, respectively. As it can be seen, in the sample prepared at 15 min the platinum particles are distributed homogeneously on S-TiO_2 surface and the Pt average particle size is 1.8 nm. The increase in the deposition time to 120 min leads to obtain an important increase in the metal particle size, thus for the platinized sample prepared with the highest deposition time (Figure 2D), the average Pt particle size was 5 nm.

The UV-Vis DRS spectra of the samples analyzed are presented in Figure 3, as it can be seen in this figure, the characteristic absorption band edge of the TiO_2 semiconductor is located at around 400 nm for all the samples; Band-gaps values were found to be located

between 3.20 and 3.21 eV without influence of the gold deposition time. After sulfation or noble metal addition the band gap value of the bare TiO_2 slightly decreases.

After the metal deposition is evident that the absorption in the visible region of 400 to 700 nm increases (Figure 3 right); thus, in the case of the Au-S-TiO_2 catalysts, in the visible part of the spectra the surface plasmon band of metallic gold could be observed at around 540 nm.

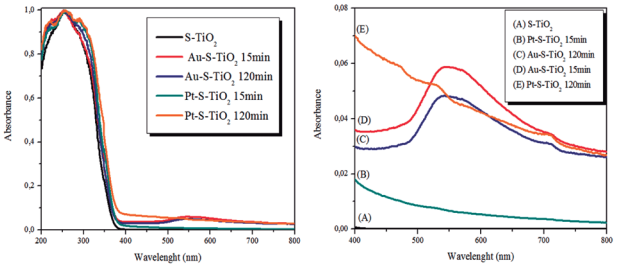

Figure 3. UV-Vis DRS spectra of photocatalysts analyzed.

In the case of the platinized samples (Pt-S-TiO_2) a slight blue-shift and a higher absorption in the visible was observed, this is mainly due to the gray color of these materials; the darker sample present the higher absorption, this sample was the prepared at 120 min of deposition time. It was also found that the band gap value of TiO_2 slightly decreases after platinum deposition i.e 2.8 eV. Different authors have reported that the TiO_2 band gap value decreases after Pt nanoparticles addition; it means that platinized titania systems exhibit photocatalytic activity in the visible range of the spectrum, where oxidized states of the metal seems to promote this visible response by photoexciting surface plasmons in the metal atom. This behavior promotes the formation of a Schottky junction between the TiO_2 and Pt nanoparticles, metal nanoparticles can act as sink for the electrons, thus leading to a higher separation efficiency of electron-hole pairs, which increased the photocatalytic efficiency [15,19].

In order to determine the valence states of the metal species on the titania surface, XPS analyzes were carried out and it was observed that in both cases gold or platinum precursors were only partially photoreduced on TiO_2 surface during the synthesis of these materials, yielding Au^0, $Au^{\delta+}$, Pt^0 and $Pt^{\delta+}$ species on Au-S-TiO_2 and Pt-S-TiO_2 photocatalysts. It was also observed that the metallic fraction increases as deposition time increases up to 120 min in all the series analyzed. By XPS was also possible to identify other species, thus, the Ti 2p core peaks exhibit a main component at around 458.4 ± 0.1 eV (Ti $2p_{3/2}$) in all the samples; representative of the Ti^{4+} ions in TiO_2 lattice. On the other hand, in the O 1s region, a peak located at 529.6 ± 0.2 eV can be observed for all the samples, assigned to oxygen atoms in the TiO_2 lattice. This peak is asymmetric with a shoulder located at higher binding energies; assigned to surface OH^- groups. These results are presented in Table 1 and selected spectra for the Pt-S-TiO_2 catalyst prepared with 0.5wt.% and 120 min of deposition time are presented in Figure 4.

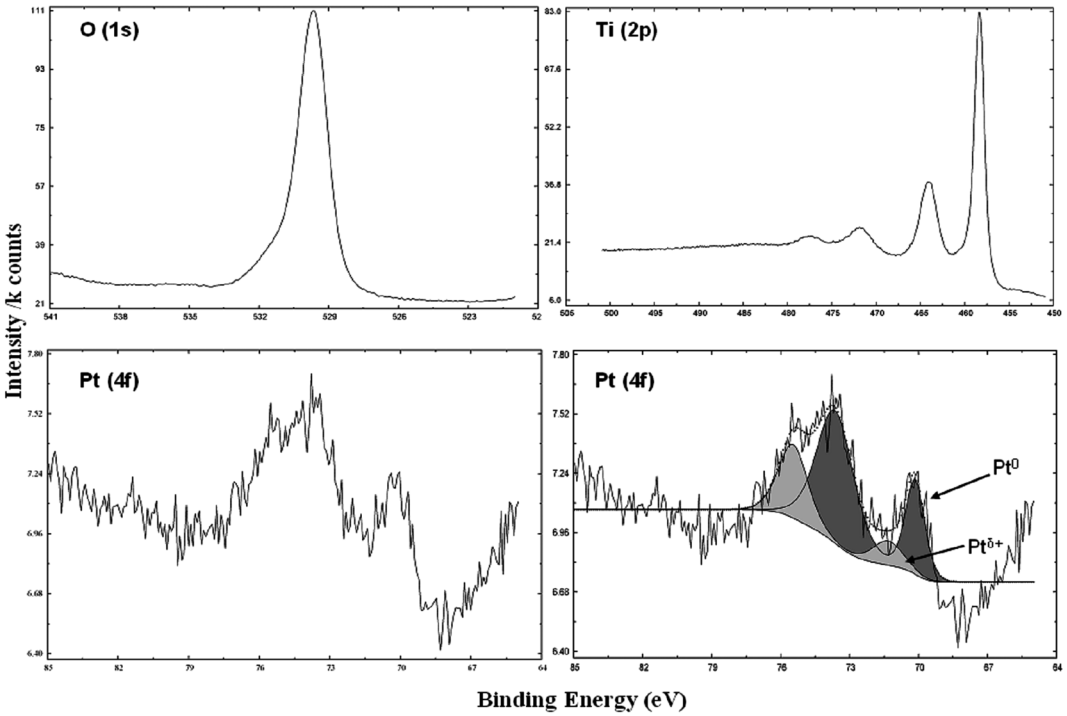

Figure 4. XPS core level spectra of O 1s, Ti (2p) and Pt (4f) regions for 0.5 wt.% Pt-S-TiO_2 synthesized at 120 min deposition time.

3.2. Methylene blue degradation over M-TiO_2 photocatalysts

In general, in the present work it was observed that the addition of 0.5 wt.% of noble metal (Au or Pt) does not modify significantly the physicochemical properties of sulfated TiO_2, as it can be seen in Table 1. Thus, as expected, the photocatalytic degradation efficiency of MB in the presence of all the samples is very similar to each other within the 2 hours of reaction time. However there are some details and or differences that worth mentioning as follows:

Figure 5 shows the evolution of methylene blue concentration during the photodegradation of this dye over S-TiO_2 and M–TiO_2 photocatalysts (M= Au or Pt). As it can be seen, dye concentration progressively decreases with the photoreaction time. No deactivation of the photocatalysts was observed even after 100 min of reaction time. The lowest MB degradation was observed by using bare TiO_2 as photocatalyst.

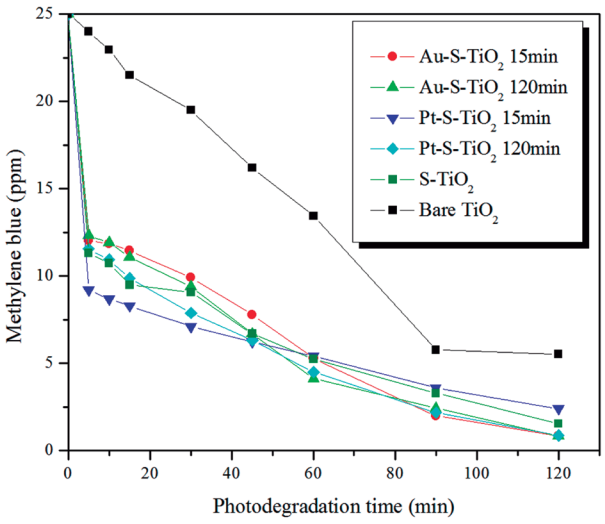

Figure 5. Evolution of the dye concentration during methylene blue photodegradation over unmetallized and metallized TiO_2 photocatalysts prepared at 15 and 120 min of deposition time.

The methylene blue degradation rate over the photocatalysts analyzed is presented in Figure 6. The dye degradation rate achieved over the bare TiO_2 catalyst was $2.28x10^{-3}$ mg Methylene blue $L^{-1}\times s^{-1}$, this value increases after sulfation and noble metal addition. The highest degradation rate was achieved over the Au-S-TiO_2 photocatalyst prepared at 120 min of deposition time. In the case of the platinized catalysts (Pt-S-TiO_2) the photocatalytic activity was higher with the catalyst prepared at 120 min of deposition time than the catalysts Pt-S-TiO_2 prepared

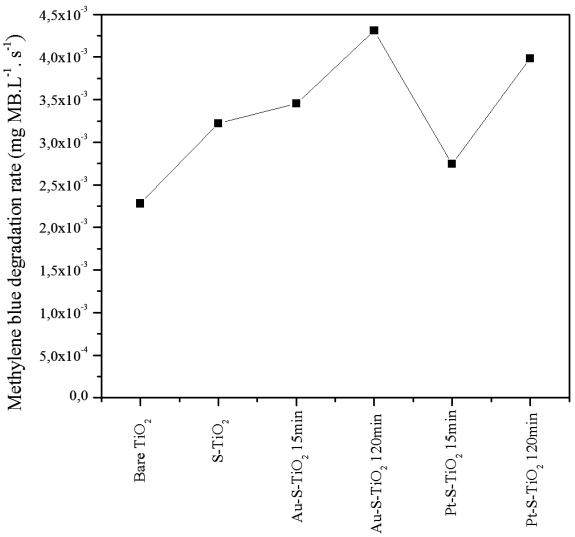

Figure 6. Methylene blue degradation rate over photocatalysts analyzed.

at 15 min of deposition time. As it can be also seen in Figure 5, the activity of this last sample is even lower than the unmetallized TiO_2 (S-TiO_2).

The increase of the TiO_2 photocatalytic degradation rate after sulfation and after gold or platinum addition can be mainly ascribed to the protective effect of sulfation, leading to a higher specific surface area, as it also been reported the oxygen vacancies generated during the sulfation and the metal deposits act as a trap for electrons, thus decreasing the recombination rate and therefore leading to a better separation of the electron–hole pairs photogenerated [9,10,15-17]; however, as it was described previously, the addition of platinum in the sample prepared with 15 min of deposition time have a detrimental effect over TiO_2 efficiency in the methylene blue degradation.

This unusual behavior can be related with the metal particle size in the materials analyzed. It has been widely reported that metal particle size strongly affects the photocatalytic activity of metallized TiO_2; thus, it is generally accepted that the addition of small metallic particles leads to better photoactivity results than the addition of large metallic particles, which can have even a detrimental effect over TiO_2 efficiency [20-22]. In the present work a very different trend was observed, since the highest methylene blue degradation rate was obtained over the metallized samples (Au or Pt-S-TiO_2) prepared with the higher deposition time; thus, the highest degradation rate was $4.31x10^{-3}$ mg of methylene blue $L^{-1}\times s^{-1}$, this value was obtained over the catalysts Au-S-TiO_2 prepared at 120 min of deposition time. Also, this catalyst presents the largest metal particle size (i.e 50 nm) among all the series

of photocatalysts analyzed (Figure 2B). On the other hand, the lowest photoactivity in the dye degradation (i.e $2.74x10^{-3}$ mg of methylene blue $L^{-1}\times s^{-1}$) was obtained over the catalyst Pt-S-TiO_2 prepared at 15 min of deposition time. In this sample the platinum particles are homogeneously distributed on S-TiO_2 surface with sizes close to 2 nm.

In order to understand the general mechanism of methylene blue degradation over the analyzed catalysts, it is important to consider the effect of the pH on the dye degradation phenomena. It has been widely reported that at pH<pzc of titania, which have been reported to be around of 6.5, the surface becomes positively charged, whereas at pH>pzc it becomes negative according to equations 2 and 3 [23,24]:

$TiOH+H^+ \Leftrightarrow TiOH_2^+$ (Equation 2)

$TiOH+OH^- \Leftrightarrow TiO^-$ (Equation 3)

The pH value in the photoreaction media is close to 4.0. Taking into account this factor, it is possible to think that: (i) Under the experimental conditions used in this work, the methylene blue adsorption is favored on positively charged TiO_2 surface; this is because methylene blue has two basic Lewis centers S and N; the aromatic rings in the molecule can also act as an electron donors to Ti(IV) species on TiO_2. (ii) The dye degradation rate increases after gold deposition on TiO_2 surface, this is because the metal particles acts as a sink for the photogenerated electrons avoiding the e^--h^+ recombination process, thus favoring the photoefficiency of titania. As it was observed, the highest photoactivity was obtained over the Au-S-TiO_2 sample prepared with 120 min of deposition time, which also exhibit the highest gold particle size. Therefore, in this catalyst the dye degradation observed can be mainly favored by a combined effect between the presence of the gold particles and a high area of the titania surface available for the methylene blue adsorption, due to the large size of the metal particles. (iii) The significant decreasing of the TiO_2 photoactivity in the methylene blue photodegradation, observed over the Pt-S-TiO_2 catalyst prepared at 15 min of deposition time can be mainly due to the high number of Pt nanoparticles covering the TiO_2 surface homogeneously, hindering the dye adsorption, thus leading to a detrimental in the methylene blue degradation rate.

4. Conclusions

In order to control the metal particle size and metal distribution in materials M-TiO_2 (M= Au or Pt) prepared by photodeposition method, the deposition times must be controlled.

The methylene blue degradation on TiO_2 significantly increases after the addition of metal nanoparticles; however, it was found that the metal particle size is an important factor influencing the M-TiO_2 photoefficiency.

Pt nanoparticles with sizes between 4 and 5 nm, has a detrimental effect in the TiO_2 photoactivity for the methylene blue photodegradation.

Au nanoparticles with the highest gold particle sizes (i.e 40-50 nm), effectively improve the methylene blue photodegradation over the Au-S-TiO_2 photocatalyst.

The highest MB degradation on Au-S-TiO_2 catalyst prepared with 120 min of deposition time can be due to the combined effect between the lower e^--h^+ recombination, induced by the presence of the metallic particles and the better MB adsorption on TiO_2 surface positively charged under acidic pH.

Acknowledgements

This work was financed by Universidad Pedagógica y Tecnológica de Colombia, Project SGI 1709 and by Fondo Nacional de Financiamiento para la Ciencia, la Tecnología y la Innovación "Francisco José de Caldas – Colciencias", Project 279-2016 and. This work was partially supported by research fund from Project Ref. CTQ2015-64664-C2-2-P (MINECO/FEDER, UE).

References

[1] M. E. Pérez, D. M. Ruiz, M. Schneider, J. C. Autino and G. Romanelli, "La química verde como fuente de nuevos compuestos para el control de plagas agrícolas". *Revista Ciencia en Desarrollo*, vol, 4 no. 2, pp.83-91, 2013.

[2] A.F. Cruz Pacheco, J. A. Gómez, "Síntesis y caracterización del sistema $La_{0,8}Sr_{0,2}MnO_3$". *Revista Ciencia en Desarrollo*, vol. 6 no. 2, pp. 133-139, 2015.

[3] E. Muñoz, J. Palacios, C. Ruis, "Microwave and ultrasound activation effect on cationization of corn and potato starches". *Revista Ciencia en Desarrollo*, vol. 4, no. 1, pp.151-173, 2012.

[4] M. Kharub, "Use of various technologies, methods and adsorbents for the removal of dye", *Journal of Environmental Research and Development,* 6, pp.879 – 883, 2012.

[5] A. Houas, H. Lachheb, M. Ksibi, E. Elaloui, C. Guillard, J-M. Herrmann, "Photocatalytic degradation pathway of methylene blue in water", *Applied Catalysis B: Environmental*, 31 pp.145–157, 2001.

[6] J.J. Murcia, M.C Hidalgo, J.A. Navío, J. Araña, J.M. Doña-Rodríguez, "Correlation study between photo-degradation and surface adsorption properties of phenol and methyl orange on TiO_2 Vs platinum-supported TiO_2", *Applied Catalysis B: Environmental*, 150–151, pp. 107– 115, 2014.

[7] S.S. Al-Shamali, "Photocatalytic Degradation of Methylene Blue in the Presence of TiO_2 Catalyst Assisted Solar Radiation", *Australian Journal of Basic and Applied Sciences,* 7(4), pp.172 – 176, 2013.

[8] J.J. Murcia, M.C. Hidalgo, J.A. Navío, V. Vaiano, P. Ciambelli, D. Sannino, "Ethanol partial photoxidation on Pt/TiO_2 catalysts as green route for acetaldehyde synthesis", *Catalysis Today*. 196, pp. 101–109, 2012.

[9] A.V. Vorontsov, E.N. Savinova, J. Zhensheng, "Influence of the form of photodeposited platinum on titania upon its photocatalytic activity in CO and acetone oxidation", *Journal of Photochemistry and Photobiology A,* 125 pp. 113–117, 1999.

[10] A.V. Vorontsov, I.V. Stoyanova, D.V. Kozlov, V.I. Simagina, E.N. Savinov, "Kinetics of the Photocatalytic Oxidation of Gaseous Acetone over Platinized Titanium Dioxide", *Journal of Catalysis,* 189 pp. 360–369, 2000.

[11] W.Y Teoh, L. Mädler, R. Amal, "Inter-relationship between Pt oxidation states on TiO_2 and the photocatalytic mineralisation of organic matters", *Journal of Catalysis,* 251, pp. 271–280, 2007.

[12] F. Denny, J. Scott, K. Chiang, W.Y. Teoh, R. Amal, "Insight towards the role of platinum in photocatalytic mineralisation of organic compounds", *Journal of Molecular Catalysis A: Chemistry,* 263, pp.93–102, 2007.

[13] C. Hu, Y. Tang, Z. Jiang, Z. Hao, H. Tang, P.K. Wong, "Characterization and photocatalytic activity of noble-metal-supported surface TiO_2/SiO_2" *Applied Catalysis A: Chemical.* 253, pp. 389–396, 2003.

[14] S. Cipagauta, J. R. Gómez, F.J Tzompantzi, A. Hernández, H. Rojas, "Síntesis Sol-gel de dióxido de titanio para el proceso de fotodegradación". *Revista Ciencia en Desarrollo,* vol. 4, no. 1, pp. 187-202, 2012.

[15] J.J. Murcia, J.A. Navío, M.C. Hidalgo, "Insights towards the influence of Pt features on the photocatalytic activity improvement of TiO_2 by platinisation", *Applied Catalysis B: Environmental,* 126, pp. 76–85, 2012.

[16] M.C. Hidalgo, J.A. Navío, J.J. Murcia, G. Colón, "Photodeposition of gold on titanium dioxide for photocatalytic phenol oxidation", *Applied Catalysis A: Chemical*, 397, pp. 112–120, 2011.

[17] G. Colón, M.C. Hidalgo, J.A. Navío, "Photocatalytic behaviour of sulphated TiO_2 for phenol degradation", *Applied Catalysis B: Environmental,* 45, pp. 39–50, 2003.

[18] K. Okazaki, Y. Morikawa, S. Tanaka, K. Tanaka, M. Kohyama, "Effects of stoichiometry on electronic states of Au and Pt supported on TiO_2 (110)", *Journal of Materials Science,* 40, pp. 3075–3080, 2005.

[19] Z. Yang, J. Lu, W. Ye, C. Yu, Y. Chang. "Preparation of Pt/TiO_2 hollow nanofibers with highly visible light photocatalytic activity", *Applied Surface Science*, 392, pp. 472–480, 2017.

[20] J. Chen, D.F. Ollis, W.H. Rulkens, H. Bruning, "Photocatalyzed oxidation of alcohols and organochlorides in the presence of native TiO_2 and metallized TiO_2 suspensions. Part (I): photocatalytic activity and pH influence", *Water Research,* 33, pp. 661–668, 1999.

[21] J.C. Crittenden, J. Liu, D.W. Hand, D.L. Perram, "Photocatalytic oxidation of chlorinated hydrocarbons in water", *Water Research,* 31, pp. 429–438, 1997.

[22] H.M. Coleman, K. Chiang, R. Amal, "Effects of Ag and Pt on photocatalytic degradation of endocrine disrupting chemicals in water", *Chemical Engineering Journal,* 113, pp. 65–72, 2005.

[23] I.K. Konstantinou, T.A. Albanis, "Photocatalytic transformation of pesticides in aqueous titanium dioxide suspensions using artificial and solar light: intermediates and degradation pathways", *Applied Catalysis B: Environmental,* 42, pp. 319–335, 2003.

[24] V.A. Sakkas, P. Calza, C. Medana, A.E. Villioti, C. Baiocchi, E. Pelizzetti, T. Albanis, "Heterogeneous photocatalytic degradation of the pharmaceutical agent salbutamol in aqueous titanium dioxide suspensions", *Applied Catalysis B: Environmental,* 77, pp. 135–144, 2007.